International Nano Letters (2019) 9:349–353
https://doi.org/10.1007/s40089-019-0280-8

SHORT COMMUNICATION

The comparison of antibacterial activities of $CsPbBr_3$ and ZnO nanoparticles

Ali Akbari[1] · Masood Mehrabian[2] · Zahra Salimi[3] · Sina Dalir[3] · Mohammadreza Akbarpour[3]

Received: 8 November 2018 / Accepted: 18 July 2019 / Published online: 25 July 2019

Abstract

All-inorganic cesium lead bromide ($CsPbBr_3$) perovskite nanoparticles and ZnO nanoparticles were synthesized. The structure, optical properties and the morphology of synthesized nanoparticles were fully characterized using X-ray diffraction (XRD), UV/Vis spectroscopy and transition electron microscopy (TEM). A comparative study was carried out to investigate the antibacterial activity of ZnO and $CsPbBr_3$ perovskite nanoparticles toward Gram-negative, rod-shaped *Escherichia coli* O157:H7 bacteria cells. Experimental results showed that the antibacterial activity of $CsPbBr_3$ nanoparticles was better than that of ZnO nanoparticles.

Keywords $CsPbBr_3$ perovskite nanoparticles · ZnO nanoparticles · Antibacterial activity · *E. coli*

Introduction

Nanotechnology is one of the most interesting branches of science which could provide materials at the nanoscale size. Nanomaterials have been utilized broadly in various fields such as tissue engineering, drug delivery, bioscience, agriculture and water due to its unique physical and chemical properties [1–3]. Recently, nanoparticles (NPs) demonstrated a high impact in the antibacterial filed [4, 5]. Among them, zinc oxide (ZnO) is considered for its photocatalytic-driven bacterial activity in which it has a broad direct band gap energy of 3.3 eV and high exciton binding energy of 60 meV [6]. Stability, good biocompatibility, low cost, and easy preparation are some of the advantages of the ZnO nanoparticle that makes it a promising antibacterial agent [4, 7]. Beside these benefits, ZnO nanoparticle also has some important drawbacks that limited its applications as an antibacterial agent such as easily losing the active sites and showing a tendency of aggregation. More importantly, ZnO with a wide band gap ($E_g = 3.3$ eV) could generate charge carriers only in the UV portion of sunlight. It must be highlighted that to overcome these shortcomings of the ZnO nanoparticle, some simple and efficient strategies have been developed [6]. However, as an alternative, designing and fabrication of new nanomaterials with low band gap energy which is important in antibacterial activities could be considered as another strategy.

Organic–inorganic hybrid perovskite nanostructures ($MAPbX_3$; $MA = CH_3NH_3$, X = Br, Cl or I) with tunable optical properties have attracted much attention. Perovskites are one of the wonderful groups of materials which demonstrate some practical properties such as high temperature superconductivity, piezoelectricity, pyroelectricity, ferroelectricity, and catalytic property [8]. Recently, as an alternative, all-inorganic perovskites ($CsPbX_3$, X = Cl, Br, I) have received tremendous consideration due to their enhanced stability and outstanding electronic properties compared to their organic–inorganic counterparts. To the best of our knowledge, there are no reports about antibacterial activity of all-inorganic perovskites. Therefore, for the first time, we investigated and compared the antibacterial activity of inorganic cesium lead bromide ($CsPbBr_3$) perovskite powder with ZnO powder against Gram-negative, rod-shaped *Escherichia coli* O157:H7 (abbreviated as *E. coli*).

✉ Ali Akbari
akbari.a@umsu.ac.ir; Aliakbari291@gmail.com

[1] Cellular and Molecular Research Center, Cellular and Molecular Medicine Institute, Urmia University of Medical Sciences, Urmia, Iran

[2] Department of Physics, Faculty of Basic Science, University of Maragheh, P.O. Box 55136-553, Maragheh, Iran

[3] Department of Materials Engineering, Faculty of Engineering, University of Maragheh, P.O. Box 55136-553, Maragheh, Iran

Experimental results showed that $CsPbBr_3$ perovskite agent was more efficient than ZnO for the destruction of bacteria.

Materials and methods

$CsPbBr_3$ perovskite nanoparticles were fabricated through the free-surfactant process. All starting materials used for $CsPbBr_3$ Perovskite NPs including lead bromide ($PbBr_2$) and cesium bromide (CsBr) were obtained from Sigma-Aldrich and used without further purification. In a typical synthesis, in a 250 mL round bottom flask containing 100 mL DMF, 1 mg $PbBr_2$ was dispersed via ultra-sonication. After stirring at 75 °C for 20 min, the appropriate amount of CsBr in ethanol was added dropwise to the mixture solution under vigorous stirring. Reaction temperature was decreased to 50 °C and stirred for 10 min. The obtained solution was centrifuged at 2500 rpm for 10 min and then washed several times with 1-propanol. Finally, collected powders were annealed at 350 °C and dried at 80 °C for 24 h [9].

In the case of ZnO NPs synthesis, zinc acetate dihydrate [$Zn(O_2CCH_3)_2{\cdot}2H_2O$], isopropanol and monoethanolamine were purchased from Sigma-Aldrich. ZnO NPs were prepared using the sol–gel pyrolysis method [10]. Typically, 1.1 g zinc acetate dihydrate was added in a mixture of isopropanol (15 mL) and monoethanolamine (0.55 mL). To obtain a clear and homogeneous solution, the mixture was stirred at 75 °C for 2 h. To make gel, the solution was kept for 2 days (aging). The gel was then preheated at 80 °C to evaporate the solvent and remove organic residuals. Finally, the obtained solid powders were annealed at 350 °C for 2 h. Shimadzu UV-1800 model spectrophotometer, SEM/EDX (MIRA3 TESCAN microscope) and TEM (Philips CM120). The agar well diffusion method was utilized to test the antibacterial property of NPs against *Escherichia coli* O157:H7 bacteria cells [11].

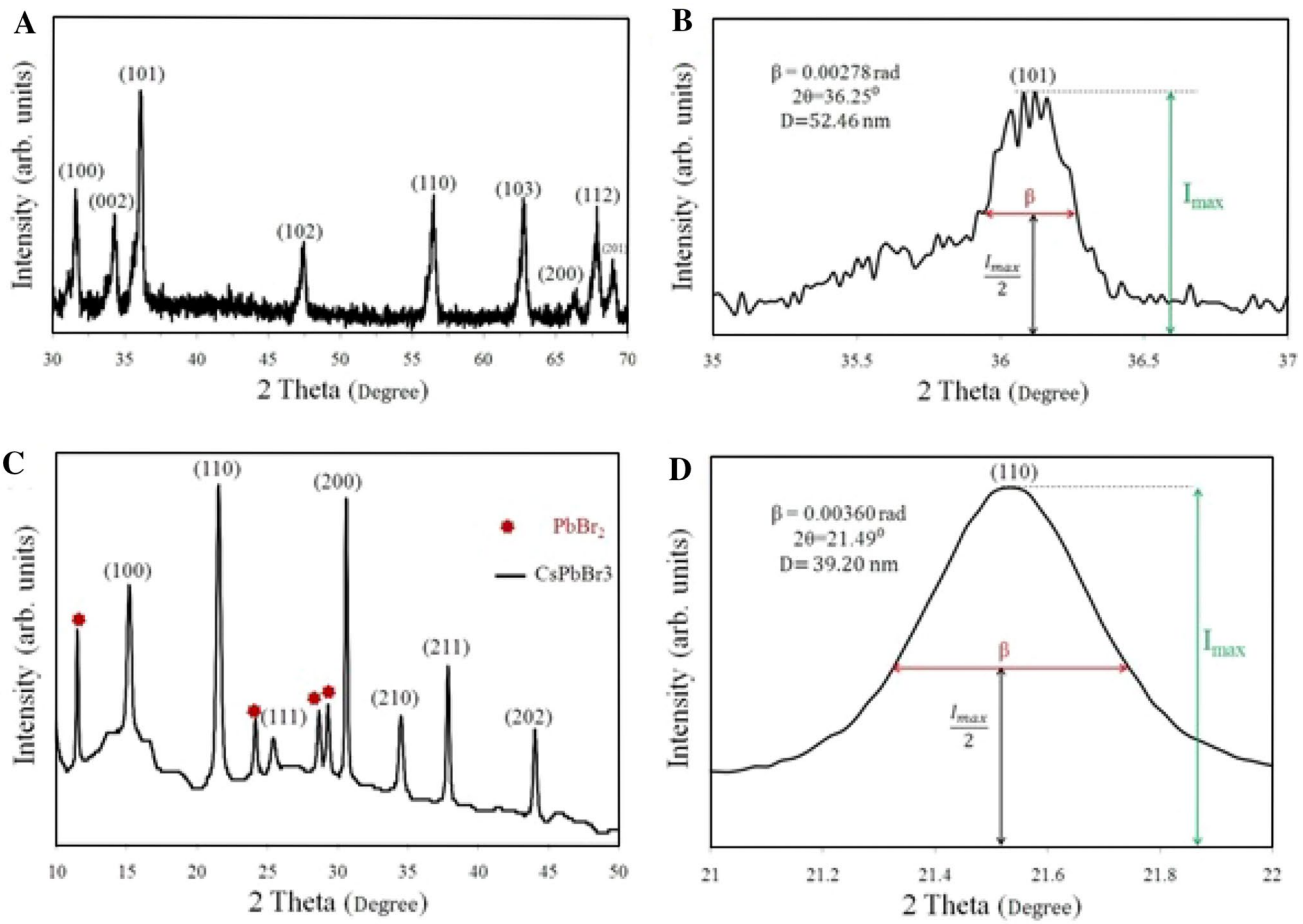

Fig. 1 **a** XRD pattern of ZnO NPs, **b** average crystalline size of ZnO NPs calculated by Scherrer's equation, **c** XRD pattern of $CsPbBr_3$ perovskite NPs, **d** average crystalline size of $CsPbBr_3$ perovskite NPs calculated by Scherrer's equation

Results and discussions

Figure 1a, c depicts the XRD patterns of ZnO NPs and $CsPbBr_3$ perovskite NPs, respectively. From Fig. 1a, the characteristic peaks at 2θ values of 31.75° (100), 34.44° (002), 36.25° (101), 47.54° (102), 56.55° (110), 62.87° (103), 66.38° (200), 67.91° (112), 69.05° (201), and 72.61° (004) can be related to the polycrystalline with wurtzite structure of ZnO (JCPS card no. 5-0664) [12]. The sharp and narrow peaks with no characteristic peaks of any impurities indicated that high-quality ZnO NPs were fabricated. The XRD pattern of $CsPbBr_3$ perovskite NPs is shown in Fig. 1c. The synthesized $CsPbBr_3$ powders show a monoclinic structure ($a = b = 0.5827$ nm and $c = 0.5891$ nm) [JCPS No. 018-0364]. This pattern is in very good agreement with other reports [13]. In addition, according to the Debye–Scherrer formula [14], the average crystallite size of ZnO NPs and $CsPbBr_3$ perovskite NPs was found to be ~ 52.46 nm and ~ 39.20 nm (Fig. 1b, d).

The optical behaviors of synthesized NPs were measured by absorption spectra in the UV/Vis wavelength range of 300–700 nm at room temperature and are illustrated in Fig. 2a. Absorption bands at 376 and 510 nm could be seen for ZnO and $CsPbBr_3$ perovskite NPs, respectively. Compared to ZnO NPs, the higher red shift in the adsorption band of $CsPbBr_3$ perovskite NPs indicated that a higher percentage of solar light can be used for electron–hole pair generation [15] which is substantial in antibacterial activity. Moreover, the optical band gaps of ZnO and $CsPbBr_3$ perovskite NPs were calculated using Tauc's equation, by plotting $(\alpha h\upsilon)^2$ versus $h\upsilon$ [16], as depicted in Fig. 2b.The calculated optical band gap energy of ZnO and $CsPbBr_3$ perovskite NPs is 3.3 and 2.4 eV, respectively. The lower band gap energy of $CsPbBr_3$ Perovskite NPs exhibited that the morphology of crystals may have various main active facets and response various excitation energy with different direct bandgaps, resulting from quantum size effect.

Figure 3a, b depict the TEM images of ZnO and $CsPbBr_3$ perovskite NPs, respectively. These images show that the synthesized nanoparticles had almost spherical shapes with smooth surfaces. The primary particle size of the ZnO and $CsPbBr_3$ powders was found to be approximately 59 nm and 40 in diameters, respectively. These diameters of particles were found to be in good agreement with XRD data (Fig. 1). Moreover, Fig. 3c, d shows the EDX spectrum of ZnO and $CsPbBr_3$ nanoparticles prepared on glass (Si/SiO_2) substrates, respectively. The elemental constitution of ZnO nanoparticles was found to have a weight percentage of 43.65 of silicon, 3.28 of zinc and 32.62 of oxygen. The EDX spectrum of $CsPbBr_3$ nanoparticles on glass substrate shows the existence of Cs, Pb, and Br elements. A ratio of 1.2:1.00:4.35 was obtained for Cs:Pb:Br elements from quantitative analysis, which is consistent with the expected composition.

Escherichia coli O157:H7 was used as a model to evaluate the antibacterial activities of ZnO and $CsPbBr_3$ perovskite NPs. As could be seen from Fig. 4, $CsPbBr_3$ perovskite NPs show better antibacterial activity than ZnO NPs. Generally, two main factors determine the antibacterial activity of agents; band gap and exciton binding energy. The exciton binding energy (between electrons and holes) can be calculated using the Bohr diameter of the nanoparticle [17]. $CsPbBr_3$ nanoparticles with a band gap of 2.4 eV and exciton binding energy (Eb) of 40 meV show a stronger antibacterial effect on *E. coli* rather than ZnO NPs with a wider band gap of 3.3 eV and larger exciton binding energy of 60 meV. The band gap determines the wavelength at

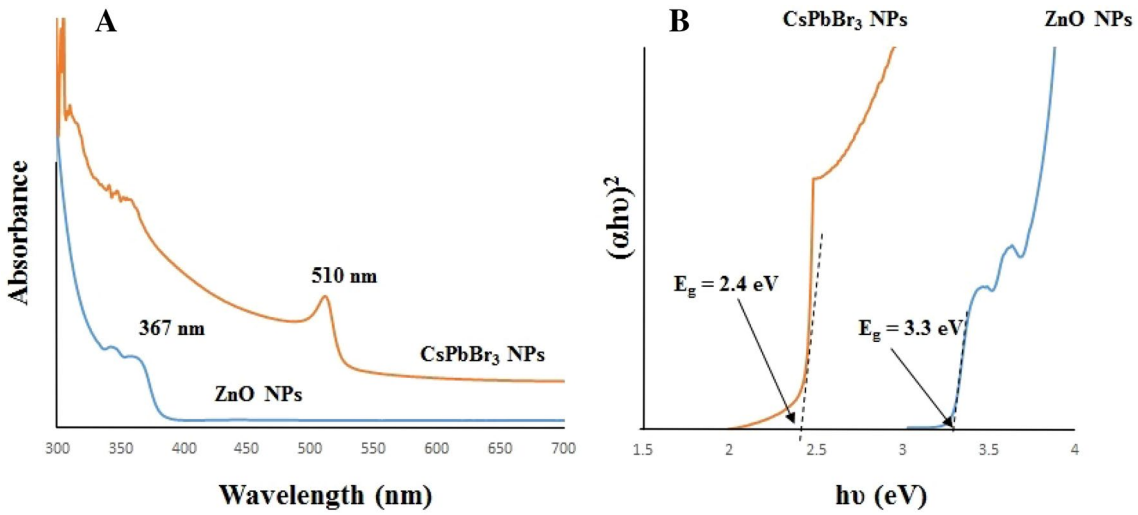

Fig. 2 **a** UV/Vis adsorption spectra of ZnO and $CsPbBr_3$ perovskite NPs and **b** Tauc plot of ZnO and $CsPbBr_3$ perovskite NPs

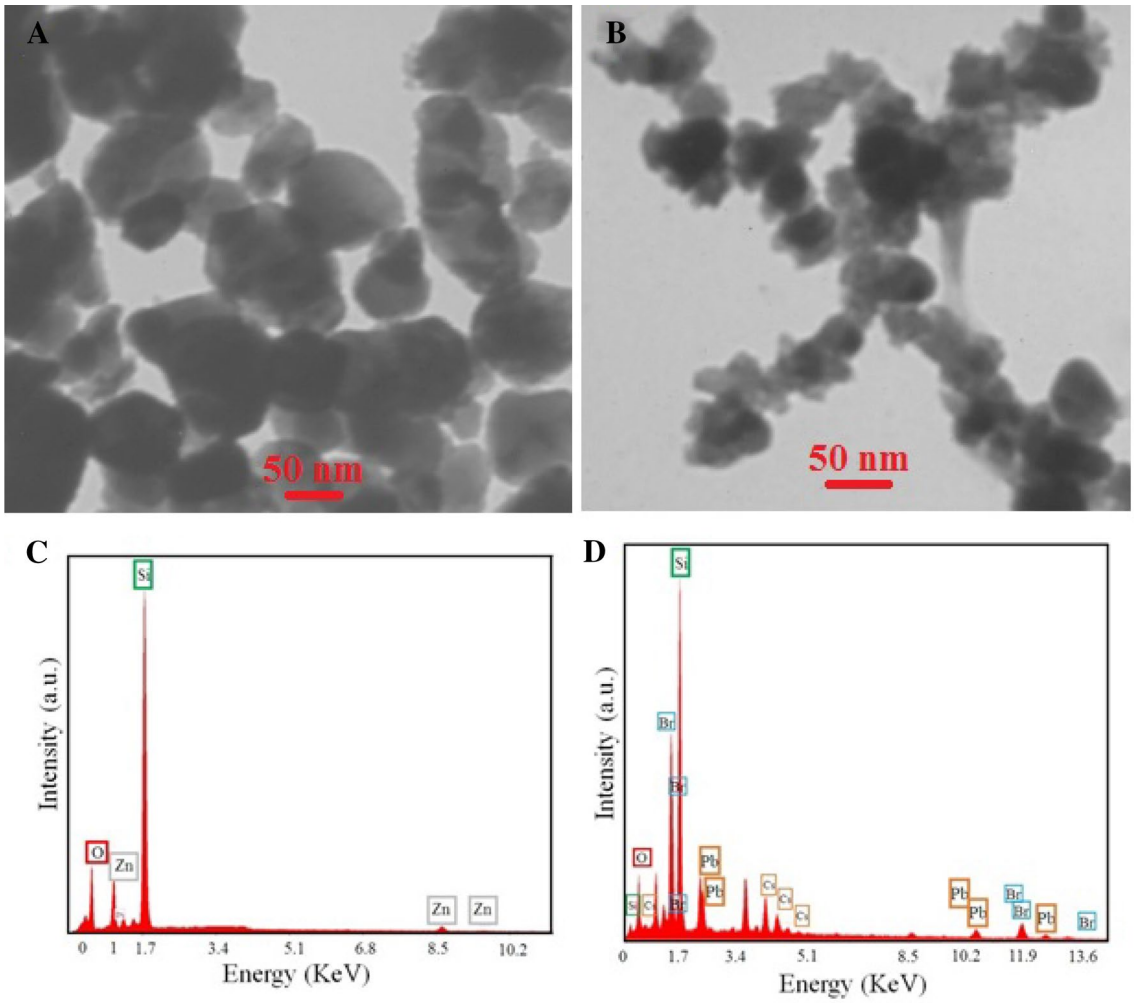

Fig. 3 TEM images of the **a** ZnO and **b** $CsPbBr_3$ nanopowders annealed at 350 °C

which the material could absorb the incident light and the wavelength at which antibacterial agents operate most efficiently. A wider band gap agent (ZnO nanoparticles) is useful only at shorter wavelengths than $CsPbBr_3$ nanoparticles. The band gaps ZnO (3.3 eV) and $CsPbBr_3$ correspond to wavelengths of approximately 375 nm and 510 nm, which is UV and visible regions, respectively. Exciton binding energy refers to the stability against thermal dissociation of excitons which have a great tendency to dissociate due to the thermal energy. In ZnO NPs, a significant number of excitons exist (higher exciton binding energy), but due to its wider band gap, only few electron–hole pairs could be created at room temperature. These two important effects determine the antibacterial activity of nanoparticles. As a result, more free created electrons and holes have sufficient lifetime in $CsPbBr_3$ which could induce photo-generation of reactive oxygen species (ROS) on the surface of $CsPbBr_3$ from adsorbed oxygen.

Conclusion

Two different types of nanoparticles, ZnO and $CsPbBr_3$ perovskite, were successfully synthesized and characterized. Free-surfactant fabrication of $CsPbBr_3$ perovskite NPs offered a fast, easy and inexpensive approach for the synthesis of nanomaterials, which show potential for antibacterial activity at a large scale. The antibacterial activity of nanoparticles against *Escherichia coli* O157:H7 was evaluated. Experimental results showed a significant room temperature antibacterial operation of $CsPbBr_3$ perovskite nanoparticles due to its narrower band gap.

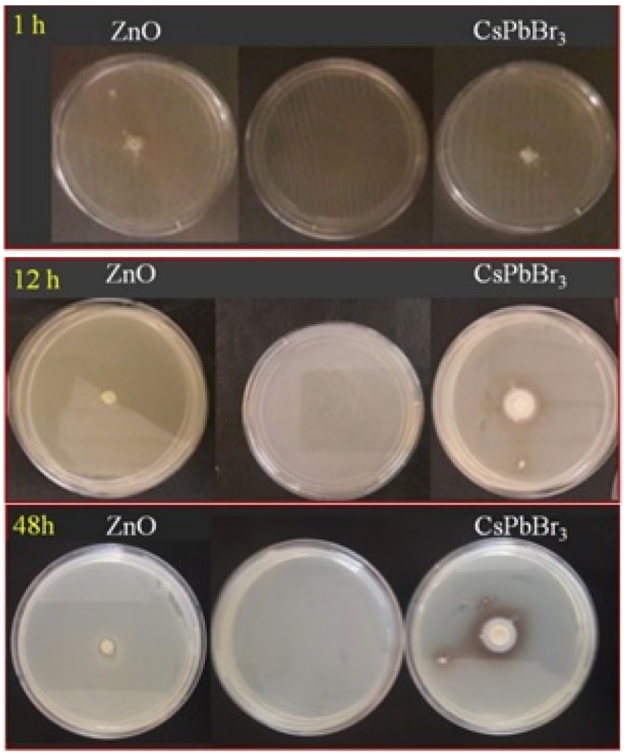

Fig. 4 Antibacterial activity of ZnO and $CsPbBr_3$ on *E. coli* treated through the well diffusion method at different periods of treatment (1, 12 and 48 h)

References

1. Santhosh, C., Velmurugan, V., Jacob, G., Jeong, S.K., Grace, A.N., Bhatnagar, A.: Role of nanomaterials in water treatment applications: a review. Chem. Eng. J. **306**, 1116–1137 (2016)
2. Sahoo, S.K., Misra, R., Parveen, S.: Nanoparticles: a boon to drug delivery, therapeutics, diagnostics and imaging. In: Nanomedicine in Cancer, pp. 73–124. Pan Stanford (2017)
3. Peters, R.J., Bouwmeester, H., Gottardo, S., Amenta, V., Arena, M., Brandhoff, P., Marvin, H.J., Mech, A., Moniz, F.B., Pesudo, L.Q.: Nanomaterials for products and application in agriculture, feed and food. Trends Food Sci. Technol. **54**, 155–164 (2016)
4. Sirelkhatim, A., Mahmud, S., Seeni, A., Kaus, N.H.M., Ann, L.C., Bakhori, S.K.M., Hasan, H., Mohamad, D.: Review on zinc oxide nanoparticles: antibacterial activity and toxicity mechanism. Nano-Micro Lett. **7**, 219–242 (2015)
5. Ghasemi, N., Jamali-Sheini, F., Zekavati, R.: CuO and Ag/CuO nanoparticles: Biosynthesis and antibacterial properties. Mater. Lett. **196**, 78–82 (2017)
6. Qi, K., Cheng, B., Yu, J., Ho, W.: Review on the improvement of the photocatalytic and antibacterial activities of ZnO. J. Alloys Comp. **727**, 792–820 (2017)
7. Iqbal, T., Khan, M., Mahmood, H.: Facile synthesis of ZnO nanosheets: Structural, antibacterial and photocatalytic studies. Mater. Lett. **224**, 59–63 (2018)
8. Noh, J.H., Im, S.H., Heo, J.H., Mandal, T.N., Seok, S.I.: Chemical management for colorful, efficient, and stable inorganic–organic hybrid nanostructured solar cells. Nano Lett. **13**, 1764–1769 (2013)
9. Du, X., Wu, G., Cheng, J., Dang, H., Ma, K., Zhang, Y.W., Tan, P.F., Chen, S.: High-quality CsPbBr 3 perovskite nanocrystals for quantum dot light-emitting diodes. RSC Adv. **7**, 10391–10396 (2017)
10. Habibi, M.H., Karimi, B.: Preparation, characterization, and application of zinc oxide nanoparticles by sol-gel pyrrolysis method: Influence of annealing temperature on crystalline phases. Synth React Inorg metal Org Nano-metal Chem **44**, 1291–1298 (2014)
11. Dobrucka, R., Długaszewska, J.: Biosynthesis and antibacterial activity of ZnO nanoparticles using Trifolium pratense flower extract. Saudi J. Biol. Sci. **23**, 517–523 (2016)
12. Akhtar, M.J., Ahamed, M., Kumar, S., Khan, M.M., Ahmad, J., Alrokayan, S.A.: Zinc oxide nanoparticles selectively induce apoptosis in human cancer cells through reactive oxygen species. Int. J. Nanomed. **7**, 845 (2012)
13. Shekhirev, M., Goza, J., Teeter, J.D., Lipatov, A., Sinitskii, A.: Synthesis of cesium lead halide perovskite quantum dots. J. Chem. Educ. **94**, 1150–1156 (2017)
14. Patterson, A.: The Scherrer formula for X-ray particle size determination. Phys. Rev. **56**, 978 (1939)
15. Bhuyan, T., Khanuja, M., Sharma, R., Patel, S., Reddy, M., Anand, S., Varma, A.: A comparative study of pure and copper (Cu)-doped ZnO nanorods for antibacterial and photocatalytic applications with their mechanism of action. J. Nanopart. Res. **17**, 288 (2015)
16. Tumuluri, A., Naidu, K.L., Raju, K.J.: Band gap determination using Tauc's plot for LiNbO3 thin films. Int. J. Chem. Tech. Res **6**, 3353–3356 (2014)
17. Jing, Q., Zhang, M., Huang, X., Ren, X., Wang, P., Lu, Z.: Surface passivation of mixed-halide perovskite CsPb (Br x I 1− x) 3 nanocrystals by selective etching for improved stability. Nanoscale **9**, 7391–7396 (2017)